Chemical Science

ROYAL SOCIETY OF CHEMISTRY

EDGE ARTICLE

View Article Online
View Journal | View Issue

Cite this: *Chem. Sci.*, 2021, **12**, 1363

All publication charges for this article have been paid for by the Royal Society of Chemistry

Received 18th September 2020
Accepted 24th November 2020

DOI: 10.1039/d0sc05192f

rsc.li/chemical-science

Arylation of *gem*-difluoroalkenes using a Pd/Cu Co-catalytic system that avoids β-fluoride elimination†‡

Kedong Yuan, [a] Taisiia Feoktistova, [b] Paul Ha-Yeon Cheong *[b] and Ryan A. Altman *[c]

Pd^{II}/Cu^{I} co-catalyze an arylation reaction of *gem*-difluoroalkenes using arylsulfonyl chlorides to deliver α,α-difluorobenzyl products. The reaction proceeds through a β,β-difluoroalkyl–Pd intermediate that typically undergoes unimolecular β-F elimination to deliver monofluorinated alkene products in a net C–F functionalization reaction. However to avoid β-F elimination, we offer the β,β-difluoroalkyl–Pd intermediate an alternate low-energy route involving β-H elimination to ultimately deliver difluorinated products in a net arylation/isomerization sequence. Overall, this reaction enables exploration of new reactivities of unstable fluorinated alkyl–metal species, while also providing new opportunities for transforming readily available fluorinated alkenes into more elaborate substructures.

Introduction

Due to the intrinsic small size and high electronegativity, incorporation of fluorine at specific positions of bio-relevant molecules can improve pharmacokinetic, pharmacodynamic and physicochemical properties, thus facilitating the drug discovery process.[1] For instance, replacing benzylic CH_2 units with CF_2 significantly influences metabolic properties, and strategies that incorporate fluorine directly into these positions aid in accessing the next generation of therapeutic candidates.[2]

Recently, tremendous effort has been devoted to develop diverse reactions for accessing fluorinated drug-like substructures. One important strategy exploits fluorinated synthons, such as *gem*-difluoroalkenes, as valuable and readily-accessible building blocks for further functionalization.[3] Relative to non-fluorinated alkenes, *gem*-difluoroalkenes show distinct reactivity trends:[4] (i) reactions typically occur at the electron-deficient *gem*-difluorinated carbon to deliver α-functionalized products (Scheme 1), (ii) anionic intermediates typically decompose *via* β-F elimination to generate mono-defluorinated products (Scheme 1A), (iii) organometallic intermediates also decompose *via* β-F elimination (Scheme 1B).[5–7] In contrast, transition metal catalysed reactions of *gem*-difluoroalkenes that avoids β-F elimination are extremely rare.[7] Such a process would require an alternate reaction pathway to avoid β-F elimination and deliver difluoroalkyl substructures (Scheme 1C). Further, a convergent preparation would complement traditional and harsh deoxyfluorination reactions of ketones that might generate this substructure.[8]

[a]*Tianjin Key Laboratory of Advanced Functional Porous Materials, Institute for New Energy Materials & Low-Carbon Technologies, School of Materials Science and Engineering, Tianjin University of Technology, Tianjin 300384, P. R. China*

[b]*Department of Chemistry, Oregon State University, 153 Gilbert Hall, Corvallis, OR, USA. E-mail: cheongh@oregonstate.edu*

[c]*Department of Medicinal Chemistry and Molecular Pharmacology, Department of Chemistry, Purdue University, West Lafayette, IN 47907, USA. E-mail: raaltman@purdue.edu*

† Dedication in Memoriam, James D. White, for his many contributions to organic synthesis.

‡ Electronic supplementary information (ESI) available. See DOI: 10.1039/d0sc05192f

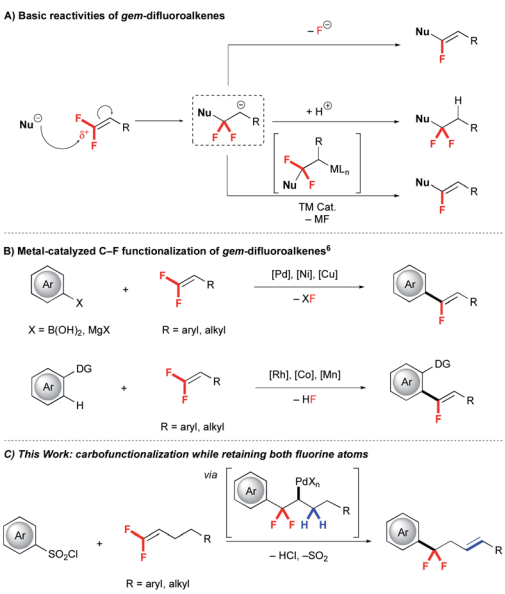

Scheme 1 Reactivity of *gem*-difluoroalkenes.

To avoid β-F elimination, we sought to offer an alternate route for the α,α-difluoroalkyl metal intermediate. Specifically, we hypothesized that β-H elimination might outcompete β-F elimination and deliver products containing both fluorine atoms. In practice, we exploited arylsulfonyl chlorides ($ArSO_2Cl$) as readily available aryl reagents that show complementary reactivity and functional group tolerance relative to aryl-halides in cross-coupling and C–H functionalization reactions.[9] These $ArSO_2Cl$ generate aryl radicals in the presence of Cu^I salts at high temperature[10] that might avoid formation of anionic intermediates. Combined, these features inspired us to explore the unique reactivity of $ArSO_2Cl$ and *gem*-difluoroalkenes using a Pd/Cu-based system. Herein, we report a Pd/Cu co-catalyzed arylation-isomerization of *gem*-difluoroalkenes that avoids β-F elimination.

Results and discussion

Optimization of reactions

Optimal reaction conditions were identified by evaluating the cross coupling of *gem*-difluoroalkene **1a** and $ArSO_2Cl$ (**2a**) to generate difluorobenzyl product **3aa** (see ESI Tables 1–7‡). Ultimately, a system of $Pd(OAc)_2$/CuCl/Li_2CO_3 was essential for generating the desired product (Table 1, entry 1), as removal of any individual component drastically decreased the yield of product (entries 2–4). In this reaction, use of an excess of **1a** suppressed the formation of side products **4**, which likely arose from Heck-arylation of alkene **3aa**. Notably, the reaction proceeded well even without ligands (entry 5), though use of an NHC ligand (SIPr·Cl) reduced the yields of side products. Eventually, optimized conditions of 5 mol% $Pd(OAc)_2$, 10 mol% SIPr·Cl, stoichiometric CuCl and Li_2CO_3 in refluxing 1,4-dioxane coupled **1a** (2.25 equiv.) and **2a** in 72% isolated yield (entry 6). Under these conditions, the difluorobenzyl group of **3aa** did not decompose to a monofluoroalkene, even at high temperature (120 °C).

Table 1 Optimization of reaction conditions[a]

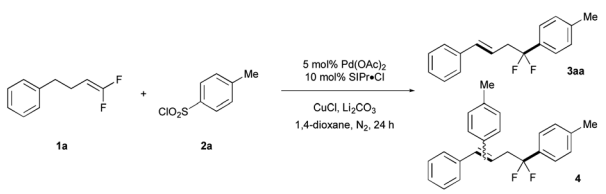

Entry	Variation from standard conditions	Conv. (%)	Yield **3aa**[b] (%)
1	None	100	78 (68)
2	No $Pd(OAc)_2$	<3	0
3[c]	No CuCl	100	16
4	No Li_2CO_3	100	0
5	No SIPr·Cl	100	75 (63)
6[d]	Reaction on 0.5 mmol, 0.33 M	100	76 (72)

[a] Conditions: **1a** (0.45 mmol), **2a** (0.20 mmol), $Pd(OAc)_2$ (0.010 mmol), SIPr·Cl (0.020 mmol), CuCl (0.24 mmol), Li_2CO_3 (0.40 mmol), 1,4-dioxane (0.50 mL, 0.40 M), N_2, reflux for 24 h. Yields were determined by GC analysis using dodecane (20 μL) as internal standard. [b] Mixture of diarylation products (<10%) were observed. Isolated yields are given in parentheses. [c] 1-(2-Chloro-1,1-difluoro-4-phenylbutyl)-4-methylbenzene and mono-defluorinated arylation products were observed. [d] Reaction was performed based on **2a** (0.50 mmol) in 0.33 M solution of 1,4-dioxane. SIPr·Cl = 1,3-bis[2,6-bis(1-methylethyl) phenyl]-1*H*-imidazolium chloride.

Evaluation of substrate scope

The reaction conditions tolerated a broad scope of $ArSO_2Cl$ bearing many important functional groups (Table 2). A variety of *para*-substituted $ArSO_2Cl$ were tolerated, including halogenated groups that are not tolerated by many Pd-catalyzed coupling reactions (I, Br, Cl; **3ab–3ad**) and electron withdrawing groups (CN, NO_2, CO_2Me; **3af–3ah**). Interestingly, benzyl chloride product **3ai** was formed in moderate yield from reaction of 4-(bromomethyl)benzenesulfonyl chloride and **1a** through an extra halogen exchange step. This benzyl electrophile would be useful for further synthetic elaboration. Fluorinated $ArSO_2Cl$ reacted smoothly to give the corresponding arylation product in good yields (**3aj–3an**). *Ortho*-substituted $ArSO_2Cl$ coupled effectively (**3al–3ao**), and heteroarylsulfonyl chlorides were tolerated albeit with reduced yields of product (**3aq–3as**). Notably, reactions of electron-rich (*e.g.* OMe, SMe, NHAc) and *N*-heteroaryl (pyridine, imidazole, pyrazole, quinoline) sulfonyl chlorides reacted in lower yield or with poor selectivity due to competing defluorination. The reaction proceeded on well on larger scales, with **3aj** obtained on 5 mmol scale without decreasing the reaction yield.

The catalytic system also coupled various aryl-substituted *gem*-difluoroalkenes (Table 3) and afforded **3ba–3da**, **3eg** and **3fa** in good yields. Reaction of alkyl-substituted *gem*-

Table 2 Scope of arylsulfonyl chlorides[a]

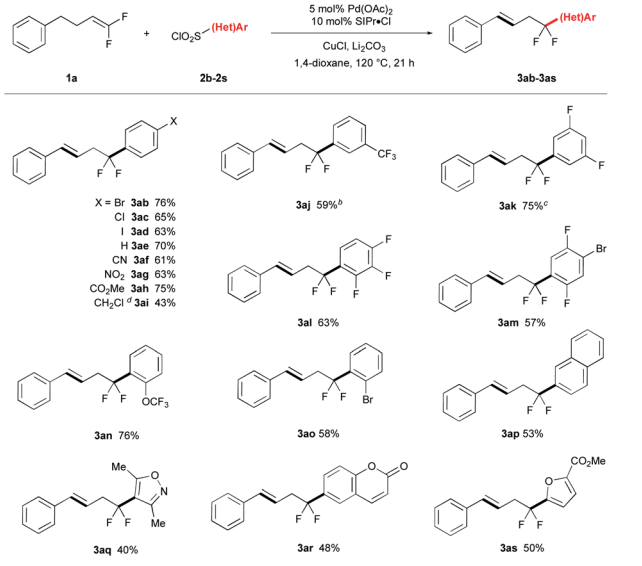

[a] Conditions: **1a** (0.875 mmol), **2** (0.50 mmol), $Pd(OAc)_2$ (0.025 mmol), SIPr·Cl (0.050 mmol), CuCl (0.60 mmol), Li_2CO_3 (1.0 mmol), 1,4-dioxane (1.5 mL), N_2, reflux for 21 h; isolated yields. [b] Reaction performed on 5.0 mmol scale of **2j**. [c] Li_2CO_3 (3.0 equiv.). [d] Start from 4-(bromomethyl)benzenesulfonyl chloride.

Table 3 Scope of *gem*-difluoroalkenes[a]

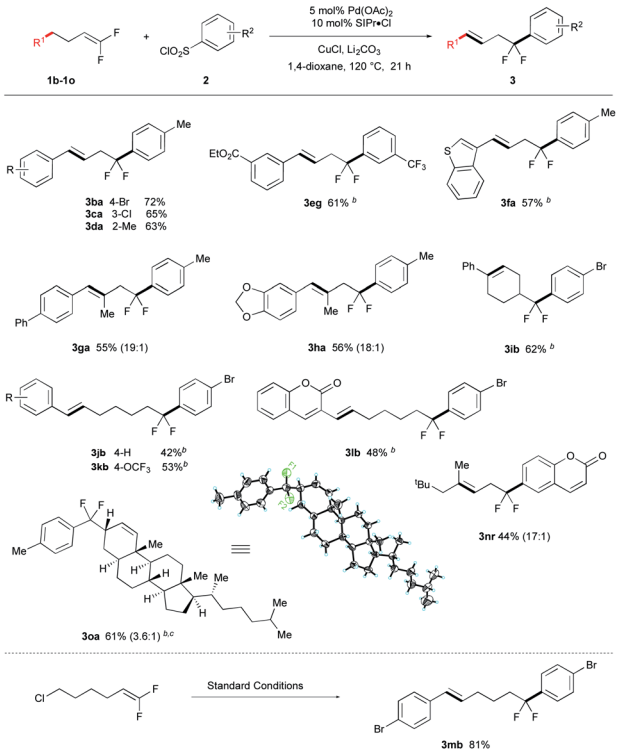

[a] Conditions: **1a** (0.875 mmol), **2** (0.50 mmol), $Pd(OAc)_2$ (0.025 mmol), SIPr·Cl (0.050 mmol), CuCl (0.60 mmol), Li_2CO_3 (1.0 mmol), 1,4-dioxane (1.5 mL), N_2, reflux for 21 h; isolated yields; selectivity was determined by ^{19}F NMR and GC analysis of crude mixture. [b] **1b**, 1.75 equiv. [c] 110 °C, reflux for 38 h. X-ray structure of **3oa** provided.

difluoroalkenes gave trisubstituted alkenes **3ga**, **3ha** and **3ib** in good stereoselectivity. Extension the aliphatic carbon chain slightly decreased the yields (**3jb–3lb**), though these reactions required additional β-hydride elimination/reinsertion steps to produce the energetically favoured products. Notably, the reaction of cholesterol derivative **1o** afforded coupled product **3oa** in 61% yield as a mixture of diastereomers (3.6 : 1), of which the relative stereochemistry was determined by X-ray crystallography (CSD: q79h).§ Finally, the reaction of 6-chloro-1,1-difluoro-hex-1-ene with **2b** afforded diarylation product **3mb**, which presumably proceed *via* a sequence involving arylation-isomerization-arylation (see figure inset).

Mechanistic investigations

A combination of computational and experimental mechanistic studies (see below) and previous literature,[10–12] support a mechanism involving Pd^{II}/Pd^{III} intermediates (Fig. 1). The cycle begins with Pd^{II} coordinating to the *gem*-difluoroalkene. Then a combination of the Pd^{II} catalyst, CuCl and Li_2CO_3 activate the $ArSO_2Cl$ to generate Ar$^{\bullet}$, which combines with Pd^{II} to generate a Pd^{III}–Ar intermediate. β-Migratory insertion of the Ar group into the *gem*-difluoroalkene would provide a Pd^{III}–alkyl intermediate. The Pd^{III}–alkyl intermediate undergoes β-H elimination preferentially over β-F elimination to generate

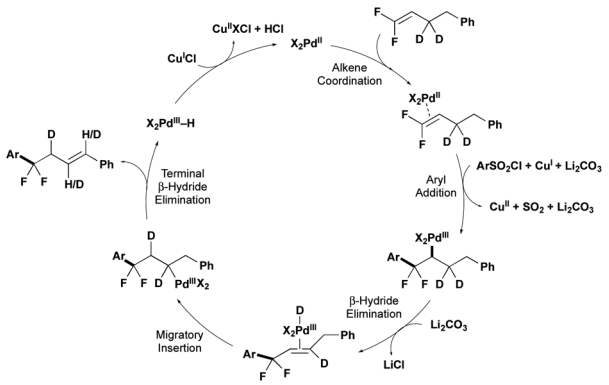

Fig. 1 Plausible mechanism for the arylation of *gem*-difluoroalkenes.

alkene-coordinated Pd^{III}–H species,[14] and subsequent hydride insertion/elimination transfers the alkene to the thermodynamically stable position, thus delivering the product that retains both fluorine atoms.

Experimental data supports early steps of the proposed cycle. First, the Pd^{II} precatalyst, Cu salt, and Li_2CO_3 are all required to activate the $ArSO_2Cl$, as the absence of any one of these components provides low conversion of $ArSO_2Cl$ (**2a**) to generate Ar–Cl and homocoupling products (Scheme 2A, Table 1, entry 4; see Table ESI-4‡ for more details). This activation

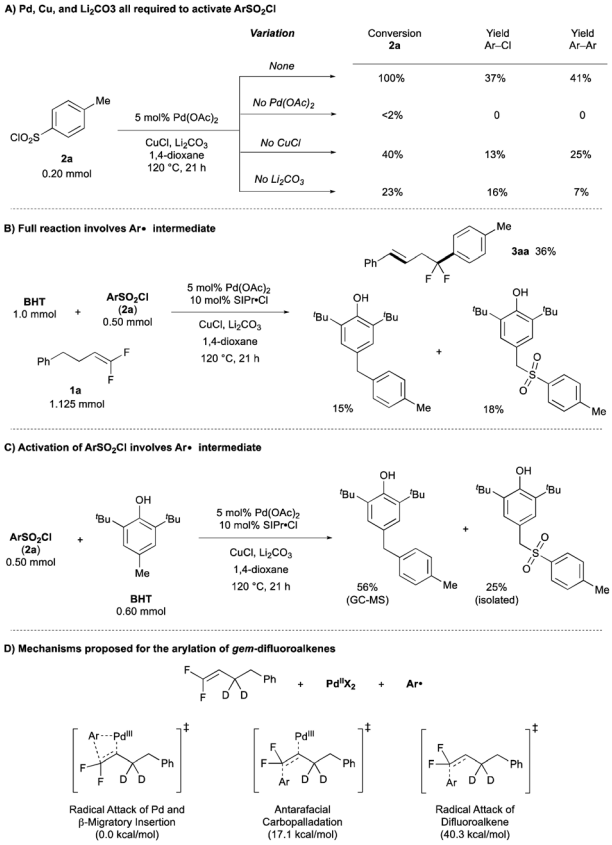

Scheme 2 Mechanistic experiments to support activation of $ArSO_2Cl$, presence of Ar$^{\bullet}$, and β-hydride elimination.

contrasts previous Cu^{I}-catalyzed reactions of $ArSO_2Cl$ that generated Ar˙ in the absence of Pd^{II} or Pd^{II}/CO_3^{2-} additives.[10a,b] Second, decomposition of $ArSO_2Cl$ generates $ArSO_2$˙ and subsequently Ar˙ intermediates, as evidenced by the generation of BHT adducts in both the full reaction (Scheme 2B) and half reaction (Scheme 2C). From this stage, the combination of the Ar˙, Pd^{II} catalyst, and *gem*-difluoroalkene could presumably react by multiple pathways (Scheme 2D; see Fig. S1‡ for more details). According to computations using density functional theory (DFT)-B3LYP-D3BJ/6-31G* & LANL2DZ/PCM (1,4-dioxane) at 120 °C, the lowest energy pathway involves a barrierless addition of the Ar˙ to Pd^{II} to generate a Pd^{III}–Ar intermediate and subsequent β-migratory insertion of the Ar group into the *gem*-difluoroalkene. In contrast, antarafacial carbopalladation of the difluoroalkene is higher in energy by 17.1 kcal mol^{-1}, while direct addition of Ar˙ to the uncoordinated *gem*-difluoroalkene to generate an unstabilized alkyl radical is 40.3 kcal mol^{-1} higher in energy.[6a,13] Of note, the Pd catalyst plays a key role in generating the unfavorable C–C bond. Specifically, while the disfavored radical attack onto the difluoroalkene (either with or without coordination to Pd^{II}) would form the new C–C bond through the arene σ-system, the Pd^{III}–Ar/β-migratory insertion pathway generates the new C–C bond through hybrid orbitals from the arene's π-system (see Fig. S1‡ for more details).

Experimental and computational experiments also confirm that β-hydride elimination can outcompete β-fluoride elimination. As evidenced by the deuterium-scrambling reaction of deuterated substrate **1q**, the reaction involves a Pd-mediated β-H elimination/reinsertion process that walks the alkene away from the difluorobenzyl moiety (Fig. 2A).[15] Computations provided additional insight into these competing processes. Overall comparison of Pd^{III} and Pd^{II} mechanisms reveals that the operative mechanism involves Pd^{III} (see Fig. S2‡): (1) β-H elimination for Pd^{III} is lower in energy than for Pd^{II} by 25.1 kcal mol^{-1}; (2) similarly, β-F elimination is favored for Pd^{III} over Pd^{II} by 37.1 kcal mol^{-1}. Interestingly, when comparing Pd^{III}- *vs.* Pd^{II}-based processes, β-H elimination is consistently favored over β-F elimination for Pd^{III}- and Pd^{II}-based mechanisms by 2.5 and 14.5 kcal mol^{-1}, respectively. Overall, for the operative Pd^{III} mechanism, β-H elimination is favored over β-F elimination by 2.5 kcal mol^{-1} (Fig. 2B). We also evaluated whether the chemoselectivity is influenced by the homobenzylic and benzylic positions of the H and F atoms by computing the elimination processes for a hypothetical substrate on which the H atoms are benzylic and F atoms are homobenzylic (see Fig. S2–S4‡ for more details). In all cases, β-H elimination is markedly preferred over β-F elimination, suggesting that the conjugation effect of the benzylic or the homobenzylic positions are not sufficiently strong to reverse the selectivity. To elucidate the origins of β-H/F elimination selectivity, distortion–interaction analysis revealed that (Fig. 2B): (1) the interaction energies were almost identical in both processes (*ca.* −54 kcal mol^{-1}); (2) the Pd^{II} catalyst was slightly more distorted at the transition state for the favoured β-H elimination (4.7 *vs.* 1.9 kcal mol^{-1}); however, (3) the substrate was significantly more distorted at the transition state for the disfavoured β-F elimination (42.7 *vs.* 36.5 kcal mol^{-1}), suggesting that the C–F bond is much stronger than the C–H bond (Fig. 2B). These results support the hypothesis that the selectivity arises from strong preference for breaking C–H bond *vs.* C–F bond.

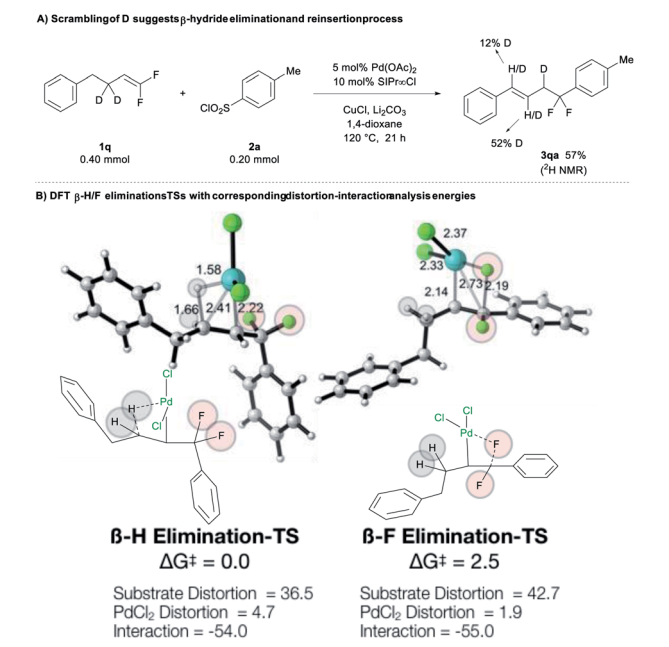

Fig. 2 Calculated β-H/F elimination transition states (TSs) with corresponding distortion-interaction analysis energies. Distances in Å and energies in kcal mol^{-1}.

Conclusions

In summary, a Pd^{II}/Cu^{I} co-catalyzed cross-coupling reaction of *gem*-difluoroalkenes and $ArSO_2Cl$ react in a net arylation/isomerization sequence that demonstrated good functional group tolerance with respect to both components and provided products bearing the "CF_2" motif at the benzylic position, which would block radical processes that might activate this position. DFT and mechanistic experiments indicate that Pd plays two key roles in the reaction, first by facilitating the formation of a challenging C–C bond, and second by reacting through a β-H elimination process, which overcomes the favoured metal-mediated β-F elimination process and delivers products bearing both fluorine atoms. These findings should enable the discovery of many complementary reactions for accessing a broad spectrum of fluoroalkyl substructures.

Conflicts of interest

There are no conflicts to declare.

Acknowledgements

We thank the National Institutes of Health (R35 GM124661) for supporting this work. NMR was provided by NIH Shared Instrumentation Grants S10OD016360 and S10RR024664, NSF

Major Research Instrumentation Grants 9977422 and 0320648, and NIH Center Grant P20GM103418. We thank Dr Victor Day for X-ray analysis and NSF-MRI grant CHE-0923449 for the X-ray diffractometer and software. We thank Mr Bo Han for helping prepare NMR files. K. Y. acknowledges support from National Natural Science Foundation of China (21702145). PHYC is the Bert and Emelyn Christensen professor of OSU, and gratefully acknowledges financial support from the Vicki & Patrick F. Stone family, and the National Science Foundation (NSF, CHE-1352663). TF acknowledges Summer Fellowship Award from the Department of Chemistry at OSU.

Notes and references

§ The crystal structure for **3oa** can be found in the Cambrige Crystallographic Data Centre under code q79h.

1 (*a*) H. J. Böhm, D. Banner, S. Bendels, M. Kansy, B. Kuhn, K. Müller, U. Obst-Sander and M. Stahl, *ChemBioChem*, 2004, **5**, 637; (*b*) E. P. Gillis, K. J. Eastman, M. D. Hill, D. J. Donnelly and N. A. Meanwell, *J. Med. Chem.*, 2015, **58**, 8315; (*c*) P. Shah and A. D. Westwell, *J. Enzyme Inhib. Med. Chem.*, 2007, **22**, 527.

2 (*a*) J. B. Xia, C. Zhu and C. Chen, *J. Am. Chem. Soc.*, 2013, **135**, 17494; (*b*) P. Xu, S. Guo, L. Wang and P. P. Tang, *Angew. Chem., Int. Ed.*, 2014, **53**, 5955; (*c*) Y. L. Xiao, Q. Q. Min, C. Xu, R. W. Wang and X. Zhang, *Angew. Chem., Int. Ed.*, 2016, **55**, 5837; (*d*) X. Li, J. Zhao, Y. Wang, J. Rong, M. Hu, D. Chen, P. Xiao, C. Ni, L. Wang and J. Hu, *Chem.–Asian J.*, 2016, **11**, 1789; (*e*) Y. Ohtsuka and T. Yamakawa, *J. Fluorine Chem.*, 2016, **185**, 96; (*f*) L. An, Y. L. Xiao, S. Zhang and X. Zhang, *Angew. Chem., Int. Ed.*, 2018, **57**, 6921.

3 (*a*) C. Liu, H. Zeng, C. Zju and H. Jiang, *Chem. Commun.*, 2020, **56**, 10442; (*b*) S. Koley and R. A. Altman, *Isr. J. Chem.*, 2020, **60**, 313; (*c*) X. X. Zhang and S. Cao, *Tetrahedron Lett.*, 2017, **58**, 375; (*d*) H. J. Tang, L. Z. Lin, C. Feng and T. P. Loh, *Angew. Chem., Int. Ed.*, 2017, **56**, 9872; (*e*) J. Hu, X. Han, Y. Yuan and Z. Shi, *Angew. Chem., Int. Ed.*, 2017, **56**, 13342; (*f*) J. Hu, Y. Zhao and Z. Shi, *Nat. Catal.*, 2018, **1**, 860.

4 (*a*) H. Amii and K. Uneyama, *Chem. Rev.*, 2009, **109**, 2119; (*b*) D. L. Orsi and R. A. Altman, *Chem. Commun.*, 2017, **53**, 7168; (*c*) D. L. Orsi, B. J. Easley, A. M. Lick and R. A. Altman, *Org. Lett.*, 2017, **19**, 1570.

5 For review see: T. Fujita, K. Fuchibe and J. Ichikawa, *Angew. Chem., Int. Ed.*, 2019, **58**, 390.

6 (*a*) X. Lu, Y. Wang, B. Zhang, J. J. Pi, X. X. Wang, T. J. Gong, B. Xiao and Y. Fu, *J. Am. Chem. Soc.*, 2017, **139**, 12632; (*b*) R. T. Thornbury and F. D. Toste, *Angew. Chem., Int. Ed.*, 2016, **55**, 11629; (*c*) W. Dai, H. Shi, X. Zhao and S. Cao, *Org. Lett.*, 2016, **18**, 4284; (*d*) L. Zhou, C. Zhu, P. Bi and C. Feng, *Chem. Sci.*, 2019, **10**, 1144; (*e*) W. Dai, J. Xiao, G. Jin, J. Wu and S. Cao, *J. Org. Chem.*, 2014, **79**, 10537; (*f*) P. Tian, C. Feng and T. P. Loh, *Nat. Commun.*, 2015, **6**, 7472; (*g*) D. Zell, U. Dhawa, V. Müller, M. Bursch, S. Grimme and L. Ackermann, *ACS Catal.*, 2017, **7**, 4209; (*h*) L. Kong, X. Zhou and X. Li, *Org. Lett.*, 2016, **18**, 6320.

7 J. Liu, J. Yang, F. Ferretti, R. Jackstell and M. Beller, *Angew. Chem., Int. Ed.*, 2019, **58**, 4690.

8 (*a*) M. Hudlický, *Org. React.*, 1988, **35**, 513; (*b*) T. Umemoto, R. P. Singh, Y. Xu and N. Saito, *J. Am. Chem. Soc.*, 2010, **132**, 18199.

9 $ArSO_2Cl$ as coupling reagents, see: (*a*) S. R. Dubbaka and P. Vogel, *J. Am. Chem. Soc.*, 2003, **125**, 15292; (*b*) S. R. Dubbaka and P. Vogel, *Chem.–Eur. J.*, 2005, **11**, 2633; (*c*) K. Yuan and H. Doucet, *Chem. Sci.*, 2014, **5**, 392; (*d*) L. Loukotova, K. Yuan and H. Doucet, *ChemCatChem*, 2014, **6**, 1303; (*e*) R. Jin, K. Yuan, E. Chatelain, J.-F. Soulé and H. Doucet, *Adv. Synth. Catal.*, 2014, **356**, 3831.

10 (*a*) Y. Amiel, *J. Org. Chem.*, 1971, **36**, 3697; (*b*) X. Zeng, L. Ilies and E. Nakamura, *J. Am. Chem. Soc.*, 2011, **133**, 17638; (*c*) X. Li, D. Liang, W. Huang, H. Zhou, Z. Li, B. Wang, Y. Ma and H. Wang, *Tetrahedron*, 2016, **72**, 8442.

11 X. Zhao and V. M. Dong, *Angew. Chem., Int. Ed.*, 2011, **50**, 932.

12 High-valent palladium in catalysis, see: (*a*) K. Muñiz, *Angew. Chem., Int. Ed.*, 2009, **48**, 9412; (*b*) P. Sehnal, R. Y. K. Taylor and L. J. S. Fairlamb, *Chem. Rev.*, 2010, **110**, 824; (*c*) A. J. Hickman and M. S. Sanford, *Nature*, 2012, **484**, 177.

13 (*a*) G. Manolikakes and P. Knochel, *Angew. Chem., Int. Ed.*, 2009, **48**, 205; (*b*) G. Maestri, M. Malacria and E. Derat, *Chem. Commun.*, 2013, **49**, 10424; (*c*) Q. Liu, X. Dong, J. Li, J. Xiao, Y. Dong and H. Liu, *ACS Catal.*, 2015, **5**, 6111.

14 For Pd^{III} species, see: (*a*) D. C. Powers and T. Ritter, *Nat. Chem.*, 2009, **1**, 302; (*b*) J. R. Khusnutdinova, N. P. Rath and L. M. Mirica, *J. Am. Chem. Soc.*, 2010, **132**, 7303. DFT calculation for C–Cl bond formation from Pd^{III}, see: (*c*) R. Jagadeesan, G. Sabapathi, J. Madhavan and P. Venuvanalingam, *Inorg. Chem.*, 2018, **57**, 6833.

15 H. T. Zhao, A. Ariafard and Z. Y. Lin, *Organometallics*, 2006, **25**, 812.